

Stellar disk destruction by dynamical interactions in the Orion Trapezium star cluster

Simon F. Portegies Zwart¹

¹*Leiden Observatory, Leiden University, Leiden, The Netherlands*

ABSTRACT

We compare the observed size distribution of circum stellar disks in the Orion Trapezium cluster with the results of N -body simulations in which we incorporated an heuristic prescription for the evolution of these disks. In our simulations, the sizes of stellar disks are affected by close encounters with other stars (with disks). We find that the observed distribution of disk sizes in the Orion Trapezium cluster is excellently reproduced by truncation due to dynamical encounters alone. The observed distribution appears to be a sensitive measure of the past dynamical history of the cluster, and therewith on the conditions of the cluster at birth. The best comparison between the observed disk size distribution and the simulated distribution is realized with a cluster of $N = 2500 \pm 500$ stars with a half-mass radius of about 0.5 pc in virial equilibrium (with a virial ratio of $Q = 0.5$, or somewhat colder $Q \simeq 0.3$), and with a density structure according to a fractal dimension of $F \simeq 1.6$. Simulations with these parameters reproduce the observed distribution of circum stellar disks in about 0.2–0.5 Myr.

Key words: N-body simulations — circum stellar disks — Orion Trapezium cluster

1 INTRODUCTION

The Trapezium cluster in the Orion nebula Huygens (1656, 1899) (later named M 42, NGC 1976) is one of the closest 412 pc (Reid et al. 2009) young ~ 0.3 Myr (85% of the stars $\lesssim 1$ Myr Prosser et al. 1994, but see also Hillenbrand (1997); Hillenbrand & Hartmann (1998)) star forming regions, composed of about 10^3 stars within a radius of ~ 3 pc (de Zeeuw et al. 1999). Even though the cluster is nearby and about to emerge from its parental molecular cloud (López-Sepulcre et al. 2013), its age, the number of members and the origin of its spatial and kinematic structure remain uncertain. Being one of the closest relatively massive young stellar systems it forms a key to understand cluster formation and early evolution.

The close proximity of the Trapezium cluster allows detailed observations of circum-stellar disk sizes using HST/WFPC2 (Vicente & Alves 2005). This size distribution is well characterized by a power-law (Vicente & Alves 2005), but the origin of this distribution remains uncertain. Dynamical interactions in young clusters have been demonstrated to be important for the sizes of circum stellar disks (Vincke et al. 2015), and the majority of protoplanetary disks are likely to be truncated by close stellar encounters. It is however, not clear whether in the Trapezium this process can still be recognized in the observed distribution of circum stellar disks. Vicente & Alves (2005) argue that: *albeit the young age of the Trapezium, and given that disk destruction*

is well underway, it is perhaps too late to tell if the present day disk size distribution is primordial or if it is a consequence of the massive star formation environment.

Here we show that the size distribution of the observed circum stellar disks is consistent with the disk size distribution that result from close encounters in young star clusters born with complex structure. We subsequently use the observed distribution of disk sizes to reconstruct the history of the dynamical and kinematic and structure of the cluster.

2 METHODS

We use the Astronomical Multipurpose Software Environment (AMUSE Portegies Zwart et al. 2009, 2013; Pelupessy et al. 2013) to carry out simulations. AMUSE allows us to generate initial conditions, combine a wide range of gravitational N -body packages and stellar evolution modules together with other physical models, and process the data.

The application script is written in python, even though the scientific production codes are written in compiled languages. In this way, the generation of initial conditions and data processing is mostly done at the relatively slow script-level, whereas the most demanding tasks are carried out with optimized code for high performance. The overhead introduced by opting for a scripting language for the data management is negligible.

Our production script starts by generating initial con-

ditions for the young star cluster. The gravitational calculations are solved using the 4th-order Hermite N -body code `ph4` (Steve McMillan, private communication), with a time-step parameter $\eta = 0.01$ and a softening of 100 AU.

During the integration of the equations of motion, we check for close approaches. When two stars happen to approach each other in a pre-determined encounter radius (initially 0.02 pc) we interrupt the N -body integrator after synchronizing the system to subsequently resolve the encounter.

2.1 The effect of encounters on disk size

The effect of the two-body encounter on the disks of both stars is solved semi-analytically. Once a two-body encounter is detected we calculate the pericenter distance, q , by solving Kepler's equation (using the kepler-module from the `Starlab` package, Portegies Zwart et al. 2001). Note that the closest approach may be well within the adopted softening radius of 100 AU. The new disk radius for a star with mass m is calculated using (Breslau et al. 2014, which was calibrated for parabolic co-planar prograde encounters):

$$r'_{\text{disk}} = 0.28q \left(\frac{m}{M} \right)^{0.32}. \quad (1)$$

Here M is the mass of the other star. This equation is also applied for calculating the new disk radius of the encountering star. These new radii are adopted only if they are smaller than the pre-encounter disk radii. This procedure does not affect the dynamics of the system in the sense that the stars are not moved, although their total mass (star plus disk) is affected before the actual pericenter passage.

In order to reduce the number of disk truncations at runtime, and therewith the number of interrupts (and synchronizations) in the N -body integration, the new encounter distance for both stars is reset to half the pericenter distance. This prevents two stars from being detected at every integration time step while approaching pericenter, which would cause the disk to be affected repeatedly during a single encounter. This procedure therefore limits the number of encounters to the most destructive one at pericenter.

2.2 The effect of encounters on disk mass

The truncated disks of the encountering stars lose mass. We estimate the amount of mass lost from each disk using

$$dm = m_{\text{disk}} \frac{r_{\text{disk}}^{1/2} - r'_{\text{disk}}{}^{1/2}}{r_{\text{disk}}^{1/2}}. \quad (2)$$

Both encountering stars may accrete some of the material lost from the other star's disk, which we calculate with

$$dm_{\text{acc}} = dm f \frac{m}{M + m}. \quad (3)$$

Here $f \leq 1$ is a mass transfer efficiency factor. Both equations are applied symmetrically in the two-body encounter, and as a consequence both stars lose some mass and gain some of what the other has lost.

After every 0.1 Myr we synchronize the gravity solver, check for energy conservation, and dump a snapshot to file for later analysis. The energy of the N -body integrator is preserved better than $1/10^8$, which is sufficient to warrant a reliable result (Portegies Zwart & Boekholt 2014).

3 RESULTS

3.1 Initial conditions

Each calculation starts by generating a realization for the N -body model: stellar masses, positions and velocities. Each star is subsequently provided with a disk of 10% of the stellar mass and with an outer radius of $r_{\text{disk}} = 400$ AU. This corresponds to the maximal disk radius observed in the Trapezium cluster (Vicente & Alves 2005). It seems a bit small compared to proto stellar disk sizes (Andrews et al. 2009, 2010), but for our calculations we only want to know if they are truncated below the maximum observed radius.

The choice of disk mass is somewhat arbitrary, but not inconsistent with observed masses of young proto-planetary disks (Williams & Cieza 2011). The mass of the initial disk is added to the stellar mass for the N -body integration. The change in disk mass due to encounters is self consistently taken into account during the integration.

Stellar masses are selected randomly from a broken power-law (Kroupa 2001) between $0.01 M_{\odot}$, and $100 M_{\odot}$ (The mean mass of this mass function $\langle m \rangle \simeq 0.396 M_{\odot}$). The positions of the stars are selected from a fractal distribution (Goodwin & Whitworth 2004) with a fractal dimension of $F = 1.2$, 1.6 and $F = 2.0$, but additional simulations were performed using the Plummer (1911) distribution. The velocities of the stars were initially scaled such that the cluster has virial ratio $Q = 0.1$, 0.3 , 0.5 , 0.7 and $Q = 1.0$. A value of $Q < 0.5$ results in rather cold initial conditions, $Q \equiv 0.5$ puts the cluster in virial equilibrium, and higher values are suitable for super-virial clusters. We varied the number of stars (from 1000 to 3500 in steps of 500) and the initial characteristic cluster radius (from 0.125 pc in steps of 2 to 1 pc).

We present an impression of the various initial conditions in Fig. 1, and the consequence of the dynamical evolution after 0.3 Myr in Fig. 2.

Every calculation was performed four times with a different random seed to generate the initial realization. In addition, the models that compared best to the observations have $R = 0.5$ pc, $Q = 0.3$ (and $Q = 0.5$), $F = 1.6$ were performed 12 times for each value of N , and with an output time-resolution of 0.02 Myr.

3.2 Disk size distribution

All calculations were stopped at an age of 1 Myr. During this period the gravitational dynamics of the stars is resolved numerically using Newtons law of motion. Close encounters result in the truncation of the circum stellar disks. Due to the absence of any other disk destruction mechanism all the evolution in the disks is the result of the dynamical encounters, and our simple disk-destruction prescription (see § 2.1).

In fig. 3 we present the size distribution of the disks from several of the simulations. To illustrate the wide range in disk distributions depending on the initial conditions of the simulations, we show one excellent comparison, and several less satisfactory cases.

The observed distribution is limited by the telescopes resolution (Vicente & Alves 2005). The pixel size in these observations is 45 AU, and they are able to resolve disks at 1.5 pixels (or 67.5 AU), although they argue that their sample is complete down to a minimum radius of 100 to 150 AU.

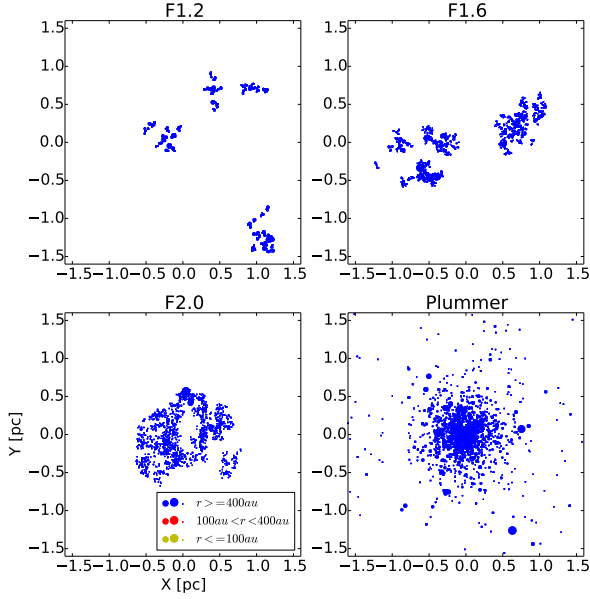


Figure 1. Initial conditions for 4 clusters, each composed of $N = 1500$ stars initially in virial equilibrium ($Q=0.5$) and distributed with a characteristic radius of 0.5 pc. From the top left to the bottom right give a fractal distribution with $F=1.2$, $F=1.6$ (top right), $F=2.0$ (bottom left) and a Plummer sphere (bottom right)

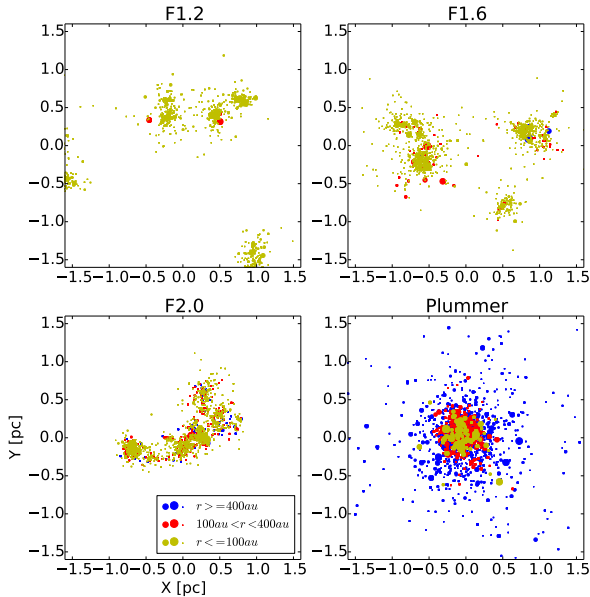


Figure 2. Presentation of four clusters from the initial conditions which we presented in Fig. 1, but evolved to 0.3 Myr. The various colors indicate the limiting radii of their disks (see bottom left for the legend).

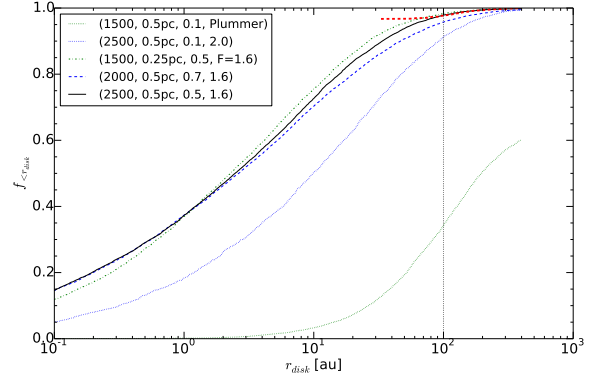


Figure 3. Cumulative radius distribution of circum-stellar disks from several simulations (see top left for the legend with number of stars N , radius R in parsec, virial temperature Q and fractal dimension F). The completeness limit in the observations at 100 AU is indicated with the vertical black dotted curve. In the simulations we are not plagued by observational selection effects. The red dotted curve gives the observed disk distribution, scaled to the model with the most comparable disk distribution (solid black curve) and with the vertical offset for disk radii ≥ 100 AU.

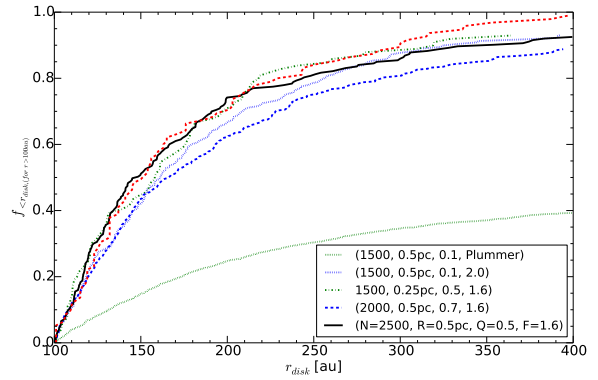


Figure 4. Cumulative size distribution of circum-stellar disks in the Trapezium cluster. The observations are complete for disk radii exceeding 100 AU. The red dotted curve gives the size distribution from the 95 observed disks. The other curves are the result of model simulations (with the legend indicating the simulation model parameters in the lower right corner). In contrast to the data presented in Tab. 1 we only show curves at an age of 0.3 Myr, whereas in the table we present the models with the highest KS- p values, which sometimes have a different age.

From the 162 proplyds 95 are larger than 100 AU (Vicente & Alves 2005). For the analysis we compare observed disk sizes with the simulated distribution of disks with a radius of at least 100 AU.

In Fig. 4 we present the cumulative distribution of disk sizes in the simulations and compare them with the observed distribution. To better compare with the observed distribution we only present here disk radii of 100 AU and larger. The degree of consistency between the observations and simulations is expressed in the p statistics of the Kolmogorov-Smirnov (Kolmogorov 1954, KS

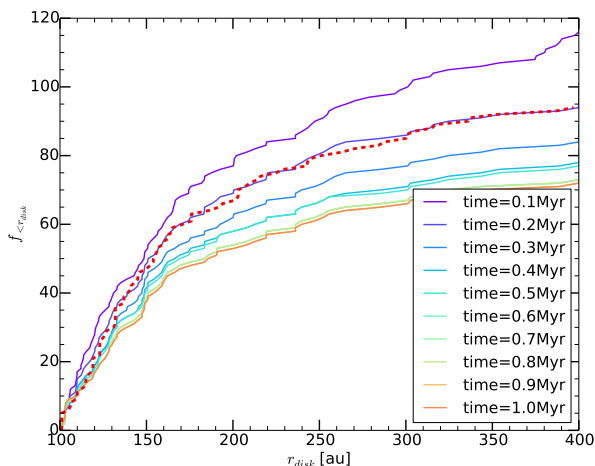


Figure 5. Time evolution of the cumulative disk-size distribution for one of our simulations with $N = 2000$ stars with $R = 0.5$ pc, $Q = 0.7$ and $F = 1.6$. This run was not included in Tab. 1, because even though this particular run gave a very satisfactory comparison with the observations, the other 3 runs did not as well and the overall value for $p = 0.024$ at $t = 0.2$ Myr. The distributions are not normalized, to show how the number of disk sizes in the observed range decreases with time. The normalized version at $t = 0.3$ Myr is also presented as the blue dashed curves in Fig. 3 (for the complete distribution) and in Fig. 4 for the normalized cumulative distribution.

hereafter), the Mann-Whitney-Wilcoxon (Mann & Whitney 1947; Wilcoxon 1945, MW hereafter) tests. For each of these tests, small values of the statistics p —say if $p \lesssim 0.05$ —we argue that the two distributions were sampled from different parent distributions, and these simulations are considered not to represent the observational data.

In Tab. 1 we present the resulting p values for the best simulations. Honestly, it is hard to make a qualitative judgment based on p values alone. We argue, however, that the number of disks with a radius ≥ 100 AU also have to be taken into account. Following Poisson statistics we argue that the observed number of disks with a radius ≥ 100 AU must be between 70 and 120 (if we do not take the statistics of the simulation into account). Several of our simulations resulted in satisfactory KS and MW statistics, but with so few (or so many) stars within the appropriate range that we could exclude them from further consideration. The remaining cases are listed in Tab. 1 (plus three ill comparisons for completeness, because those are presented also in figs. 3 and 4).

We demonstrate the evolution of the number of stars with disks $r_{\text{disk}} \geq 100$ AU in Fig. 5, where we present the time evolution of the distribution of disk sizes for one of the simulations. At an age of $t = 0.2$ Myr the disk size distribution compares well with the observed distribution, in shape as well as in number. At later age the number of stars with disks in the appropriate regime drops quite dramatically.

In Fig. 6 we present the time evolution of several simulations with a characteristic radius of $R = 0.5$ pc, a virial temperature of $Q = 0.5$ and fractal dimension $F = 1.6$. Those simulations generally result in the highest p values

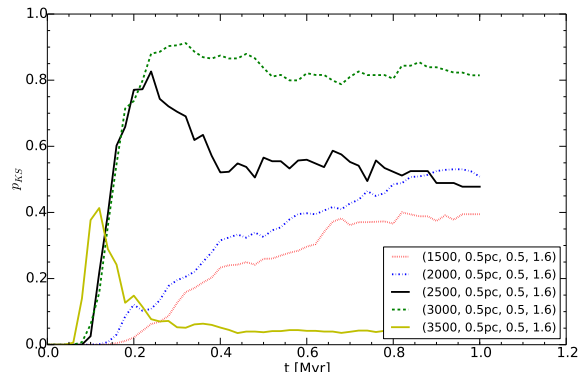


Figure 6. Kolmogorov-Smirnov p value for simulation with $N = 1500$ to $N = 3500$ stars with $R = 0.5$ pc, $Q = 0.5$ and fractal dimension $F = 1.6$ up to an age of 1 Myr. The KS values are calculated by summing over 12 runs for each set of parameters with a time resolution of 0.02 Myr.

for KS statistics (and equivalently so for for MW statistic) in comparison with the observed circum stellar disk-size distribution.

The runs with $N = 1000$ and 2000 show a steady but relatively slow rise to a KS probability $p \simeq 0.5$ on a time scale of about 1 Myr, and the high $N = 3500$ simulation peaks at $t \simeq 0.1$ Myr but hardly exceeds $p = 0.4$. The simulations with intermediate N (between 2500 and $N = 3000$) show a promising trend of peaking around $t = 0.2$ – 0.3 with a maximum $p \sim 0.9$.

3.3 Disk mass distribution

Disk masses have been determined in the Orion Trapezium cluster using millimeter observations (Mann & Williams 2009). This has been calculated from the spectral energy distribution from centimeter to submillimeter wavelengths and of the interferometric response to the cloud background for 26 out of 55 HST-identified proplyds (Mann & Williams 2009). They show that the number of disks per logarithmic mass interval is approximately constant over almost a decade in mass between 4.2 and 35.6 M_{Jupiter} . Because these disks were selected to have bright millimeter emission, the sample is biased toward relatively large disks between 20 and 200 AU (Mann & Williams 2009). Our rather limited understanding of the initial disk mass, the radial density profile and therefore of the effect of encounters on these disks, limits the validity of comparing the observations with the simulations.

In Fig. 7 we present the cumulative mass distribution of several simulations and compare them with the observed mass distribution. Apart from the Plummer initial conditions, it appears to be difficult to exclude any of the model simulation in Tab. 1. Our assumption of an initial disk mass of 10% of the zero-age stellar mass is quite arbitrary. If we would have adopted half this value, the curves in Fig. 7 skew somewhat to the left the tree overlapping curves (black, blue dashed and green dash-dotted curves) just staying above the observed distribution, whereas the blue dotted curve

Table 1. Results of the simulations. The top 9 rows give the initial conditions for the simulations which compare best with the observations. The bottom three rows give the results of additional simulations, for which the data is also presented in the accompanying figures. The first two column gives the number of stars and the time (in Myr) at which the snapshot was compared with the observations. The following columns give the initial radius of the cluster (in parsec), the virial ratio and the fractal dimension. The subsequent three columns give the KS and NW p values for the comparison between the observed disk distribution and the simulations, and the number of stars with a disk radius ≥ 100 AU, which corresponds to the observational limit. The last two columns give the KS p value for the comparison between the observed and simulated disk mass, and the number of disks in the simulations which comply to the observed limits ($m > 4.2M_{\text{Jupiter}}$, $20 \text{ au} < r < 200 \text{ au}$, see § 3.3).

N	t/Myr	R/pc	Q	F	$p_{r,\text{KS}}$	$p_{r,\text{NW}}$	$N_{r \geq 100 \text{ au}}$	$p_{m,\text{KS}}$	$N_{20 < r < 200 \text{ au}}$
2000	0.1	0.25	0.1	2.0	0.80	0.40	86 ± 19	0.30	236 ± 17
2500	0.1	0.25	0.1	2.0	0.84	0.39	93 ± 37	0.32	315 ± 52
2500	0.2	0.5	0.1	1.6	0.77	0.43	80 ± 24	0.50	145 ± 5
1500	0.3	0.5	0.3	1.6	0.72	0.22	78 ± 23	0.48	156 ± 30
2500	0.4	0.5	0.3	1.6	0.68	0.34	74 ± 27	0.58	193 ± 14
3000	0.3	0.5	0.3	1.6	0.70	0.50	67 ± 6	0.77	213 ± 10
2000	0.6	0.5	0.5	1.6	0.82	0.25	63 ± 9	0.76	155 ± 15
3000	0.2	0.5	0.5	1.6	0.54	0.46	80 ± 25	0.63	223 ± 30
1500	1.0	0.5	1.0	1.6	0.50	0.29	72 ± 25	0.46	144 ± 11
2000	0.2	0.5	0.7	1.6	0.02	0.01	95 ± 29	0.30	169 ± 28
1500	0.3	0.25	0.5	1.6	0.86	0.47	25 ± 10	0.66	90 ± 14
1500	0.3	0.5	0.1	Pl	0.00	0.00	986 ± 23	0.05	353 ± 17

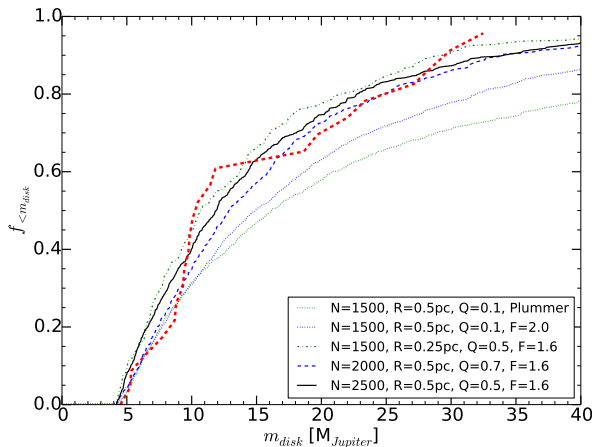


Figure 7. Cumulative distribution of disk masses in the Trapezium cluster (using $f = 1$ in Eq. 3). The observations are claimed to be complete down to a mass of $4.2 M_{\text{Jupiter}}$, below which we do not plot any data. There are only 23 observed disks with at least this mass. The other curves give the result of the model simulations at an age of 0.3 Myr; the legend (bottom right) explains the initial model parameters, but they are the same as in Fig. 3 and 4. Except the two dotted curves (green and blue), each of these models produce a satisfactory fit to the observed disk masses. Due to the limited statistics, the disk mass distribution generally compares much better to the observations than the disk size distribution.

($N=1500$, $R=0.5\text{pc}$, $Q=0.1$, $F=2.0$) compares best with the observations.

In Fig. 8 we compare the mass functions for the all stars with those with a selected disk sizes and masses. Stars with a massive disk ($m_{\text{disk}} > 4.2 M_{\text{Jupiter}}$) have considerably higher mass ($\langle m \rangle \simeq 0.34 M_{\odot}$) whereas those with a relatively

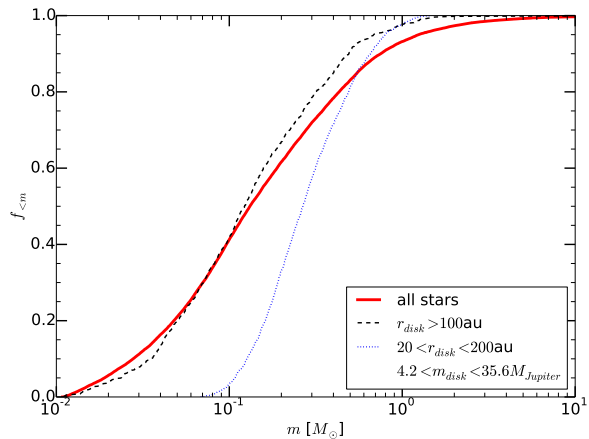


Figure 8. Cumulative distribution of stellar masses in simulation with $N = 2000$ stars, $R = 0.5 \text{ pc}$, $Q = 0.5 \text{ pc}$ and $F = 1.6$ at an age of 0.3 Myr. The red solid curve gives the mass function for all stars, and is identical to the initial mass function adopted for all our simulations. The black dashed curve give the mass function for the stars with a disk $r_{\text{disk}} > 100 \text{ AU}$, and the blue dotted curve for the stars with a disk size between 20 and 200 AU and with a disk mass between $4.2 M_{\text{Jupiter}}$ and $35.6 M_{\text{Jupiter}}$.

large disk ($r_{\text{disk}} > 100 \text{ au}$) tend to be somewhat less massive than average ($\langle m \rangle \simeq 0.22 M_{\odot}$).

The majority of simulations with rather cold initial temperature ($Q = 0.1$) fail to reproduce the observed disk distribution. Exceptions are simulations born with a fractal dimension of 1.6, which is also preferred for the disk size distribution. Most simulations with a virial temperature of $Q = 0.3$ and $Q = 0.5$ provide a satisfactory comparison with the observations.

4 DISCUSSION AND CONCLUSIONS

We have performed simulations of self gravitating stellar systems in which we incorporated a semi-analytic prescription for the effect of encounters on the sizes and masses of circumstellar disks. Our simulations aim at reproducing the disk size distribution observed around 95 stars in the Trapezium cluster (Vicente & Alves 2005) and with the 23 observed disk masses (Mann & Williams 2009).

Our simulations ignore most physical effects that tend to play an important role in the evolution of these systems, these include the presence of residual gas from the parent molecular cloud, the tidal field of the Galaxy, primordial binaries and mass segregation, stellar evolution and feedback process. The only aspect we take into account properly in our simulations are the gravitational encounters between stars. We estimate, at run time, how circum stellar disks are truncated as a result of two-body encounters. Regardless of the limited physics in our simulations the resulting disk-size distribution compares excellently with the observations. The disk mass distribution gives a consistent picture, but is less constraining due to the smaller number of observed masses. Bolstered by our success to reproduce the observed disk radius distribution from the simple argument that this distribution originates from close encounters in the young star clusters, we use this argument to limit some of the structure parameters of the cluster at an earlier age.

The disk-size distribution appears to match the observations best if the Trapezium cluster was born virialized ($Q = 0.5$) or slightly colder ($Q = 0.3$) and with a half-mass (or characteristic) radius of $R \simeq 0.5$ pc. Due to the large run-to-run variations it is hard to constrain these values further. With these parameters the best comparison is achieved for clusters with $N = 2500$ to 3000 stars.

Simulations with a smaller number of stars tend to under produce the number of stars in the range where disks have been observed, whereas in more massive cluster disks tend to be harassed on too short a time scale.

We exclude a Plummer sphere as the initial density profile, irrespective of the initial cluster radius, because too few disks are truncated. Even with cold initial conditions $Q = 0.1$ and a tiny radius $R = 0.125$ the Plummer sphere will always have some stars that remain insufficiently affected by dynamical encounters within the available time. For similar reasons we also exclude the density distribution with a relatively high fractal dimension $F \gtrsim 2$, and cluster with a large characteristic radius of $R \gtrsim 0.7$ pc, irrespective of the kinematic temperature of the initial cluster. Clusters with a fractal initial distribution of stars, with relatively cold initial conditions or a small characteristic radius $R \lesssim 0.3$ pc are also excluded, because they truncate too many disks too effectively.

An initial density distribution generated using a fractal dimension of $F = 1.6$ result in the best comparison with the observations, although the number of stars should then be between $N = 2500$ and 3000, the virial temperature of $Q \simeq 0.3$ – 0.5 , and with a half mass radius of $R \simeq 0.5$ pc.

These results are robust against small changes in the initial conditions. Additional simulations with a Salpeter mass function with a lower mass limit of $0.1 M_{\odot}$, have no appreciable effect on the results. Our prescription for the mass evolution in close encounterd depends on the initially adopted

disk size, for which we adopted 400 AU. We performed additional simulations with initial disk radii of 1000 AU, but this had no appreciable effect on the resulting disk mass size distribution.

We have not studied the effect of primordially mass-segregation, but we think that the effect somewhat mimics the a slight reduction in the initial kinematic temperature. It could therefore be preferable to start with slightly warmer initial distributions if the degree of initial mass segregation is appreciable.

The distributions of disk sizes and masses for stars that have escaped the cluster are not appreciably different than those that remain bound, irrespective of the age of the cluster. Stars tend to escape after a strong encounter and the disks have already been truncated by that time.

4.1 Further considerations

The Solar system may have been truncated at about 35 AU by a close encounter with another star (Jílková et al. 2015). According to our calculations a truncation between 10 AU and 100 AU occurs in about 25% of the planetary systems born in a cluster with parameters similar to the Trapezium cluster. The parameters of the Trapezium clusters, as constrained by our calculations, are not inconsistent with the possible parameters of the cluster in which the Sun was born (Portegies Zwart 2009), although there the anticipated cluster was slightly larger, 2 ± 1 pc and probably somewhat more massive ($2000 \pm 1000 M_{\odot}$). We still favor this larger cluster radius for forming the Solar System, because of the need to also survive the ablation of the protoplanetary disk by the ablation of supernovae. This process happens at a somewhat later time ($\gtrsim 5$ Myr), and is not accounted for in our simulations.

With the parameters that give a best comparison with the Trapezium cluster, $\sim 70\%$ of disks are truncated below ~ 10 AU within the first few hundred thousand years of their dynamical evolution. Further truncation may be initiated by photoevaporation of the massive stars in the young cluster Adams et al. (2004), but that does not effect the earliest evolution studied here. Violent disk truncation may not particularly hinder the planet formation process, but it sure excludes the formation of planets in orbits beyond the disk truncation radius. Another aspect of the truncation of protoplanetary disks may be the exclusion of Earth-like ice giants, which are expected to form well beyond the ice line ($a \gtrsim 10$ AU), and subsequently sink closer to the star in the remaining disk via what is called the grand tack model (Morbidelli et al. 2014; Deienno et al. 2015)

In a recent study Vincke et al. (2015) conclude that mutual stellar encounters are responsible for truncating protoplanetary disks in young small clusters; in clusters with an average density of 60 star/pc^3 , such as the Orion nebula cluster, up to 65% of protoplanetary disks are truncated below 1000 AU, whereas 15% is truncated even below 100 AU. In a more dense environment (500 star/pc^3) these fractions increase to 85% and 39%. Our calculations are consistent with the analysis of Vincke et al. (2015), but in order to reproduce the disk-size distribution observed in the Orion Trapezium cluster the initial cluster density has to be much higher, $\sim 10^3 \text{ star/pc}^3$.

It is interesting to note that all stars in the simulations

that reproduced the disk-size distribution observed in the Orion Trapezium cluster have captured some material from the disks of other stars. In our most favorite simulation for the Trapezium cluster ($N = 2000$, $R = 0.5$ pc, $Q = 0.5$, $F = 1.6$), about 60% of the stars have captured $\gtrsim 1\%$ of their own disk mass from another star in a close encounter, and $\sim 34\%$ captured more than 10% of mass. This is consistent with the idea proposed by Jílková et al. (2015) for the origin of the planetesimal Sedna, being captured from another star in the early evolution of the Solar System.

ACKNOWLEDGMENTS

We thank Anthony Brown, Michiel Hogerheijde, Lucie Jílková and Igas Snellen for discussions. This work was supported by the Netherlands Research Council NWO (grants #643.200.503, #639.073.803 and #614.061.608) by the Netherlands Research School for Astronomy (NOVA). The numerical computations were carried out on the Little Green Machine at Leiden University.

REFERENCES

- Adams, F. C., Hollenbach, D., Laughlin, G., Gorti, U. 2004, *ApJ* , 611, 360
- Andrews, S. M., Wilner, D. J., Hughes, A. M., Qi, C., Dullemond, C. P. 2009, *ApJ* , 700, 1502
- Andrews, S. M., Wilner, D. J., Hughes, A. M., Qi, C., Dullemond, C. P. 2010, *ApJ* , 723, 1241
- Breslau, A., Steinhausen, M., Vincke, K., Pfalzner, S. 2014, *A&A* , 565, A130
- de Zeeuw, P. T., Hoogerwerf, R., de Bruijne, J. H. J., Brown, A. G. A., Blaauw, A. 1999, *AJ* , 117, 354
- Deienno, R., Gomes, R. S., Morbidelli, A., Walsh, K. J., Nesvorný, D. 2015, in *AAS/Division of Dynamical Astronomy Meeting*, Vol. 46 of *AAS/Division of Dynamical Astronomy Meeting*, #300.04
- Goodwin, S. P., Whitworth, A. P. 2004, *A&A* , 413, 929
- Hillenbrand, L. A. 1997, *AJ* , 113, 1733
- Hillenbrand, L. A., Hartmann, L. W. 1998, *ApJ* , 492, 540
- Huygens, C. 1656, ..., ...
- Huygens, C. 1899, *Christiaan Huygens, Oeuvres complètes*, Tome VIII. Correspondance 1676-1684, Martinus Nijhoff, Den Haag (Ed. Johannes Bosscha jr.)
- Jílková, L., Portegies Zwart, S., Pijloo, T., Hammer, M. 2015, *MNRAS* , 453, 3157
- Kolmogorov, A. N. 1954, *Dokl Akad. Nauk SSSR*, 98, 527
- Kroupa, P. 2001, *MNRAS* , 322, 231
- López-Sepulcre, A., Kama, M., Ceccarelli, C., Dominik, C., Caux, E., Fuente, A., Alonso-Albi, T. 2013, *A&A* , 549, A114
- Mann, H., Whitney, D. 1947, *Annals of Mathematical Statistics*, 18, 50
- Mann, R. K., Williams, J. P. 2009, *ApJL* , 694, L36
- Morbidelli, A., Gaspar, H. S., Nesvorný, D. 2014, *Icarus* , 232, 81
- Pelupessy, F. I., van Elteren, A., de Vries, N., McMillan, S. L. W., Drost, N., Portegies Zwart, S. F. 2013, *A&A* , 557, A84
- Plummer, H. C. 1911, *MNRAS* , 71, 460
- Portegies Zwart, S., Boekholt, T. 2014, *The Astrophysical Journal Letters*, 785(1), L3
- Portegies Zwart, S., McMillan, S., Harfst, S., Groen, D., Fujii, M., Nualláin, B. Ó., Glebbeek, E., Heggie, D., Lombardi, J., Hut, P., Angelou, V., Banerjee, S., Belkus, H., Fragos, T., Fregeau, J., Gaburov, E., Izzard, R., Jurić, M., Justham, S., Sottoriva, A., Teuben, P., van Bever, J., Yaron, O., Zemp, M. 2009, *New Astronomy*, 14, 369
- Portegies Zwart, S., McMillan, S. L. W., van Elteren, E., Pelupessy, I., de Vries, N. 2013, *Computer Physics Communications*, 183, 456
- Portegies Zwart, S. F. 2009, *ApJL* , 696, L13
- Portegies Zwart, S. F., McMillan, S. L. W., Hut, P., Makino, J. 2001, *MNRAS* , 321, 199
- Prosser, C. F., Stauffer, J. R., Hartmann, L., Soderblom, D. R., Jones, B. F., Werner, M. W., McCaughrean, M. J. 1994, *ApJ* , 421, 517
- Reid, M. J., Menten, K. M., Zheng, X. W., Brunthaler, A., Moscadelli, L., Xu, Y., Zhang, B., Sato, M., Honma, M., Hirota, T., Hachisuka, K., Choi, Y. K., Moellenbrock, G. A., Bartkiewicz, A. 2009, *ApJ* , 700, 137
- Vicente, S. M., Alves, J. 2005, *A&A* , 441, 195
- Vincke, K., Breslau, A., Pfalzner, S. 2015, *A&A* , 577, A115
- Wilcoxon, F. 1945, *Biometrics Mulletin*, 1, 80
- Williams, J. P., Cieza, L. A. 2011, *ARA&A* , 49, 67